Hydrodynamic Attractor in Ultracold Atoms

Keisuke Fujii[1, 2, *] and Tilman Enss[2]

[1] *Department of Physics, The University of Tokyo, 7-3-1 Hongo, Bunkyo-ku, Tokyo 113-0033, Japan*

[2] *Institut für Theoretische Physik, Universität Heidelberg, Philosophenweg 19, 69120 Heidelberg, Germany*

The hydrodynamic attractor is a concept that describes universal equilibration behavior in which systems lose microscopic details before hydrodynamics becomes applicable. We propose a setup to observe hydrodynamic attractors in ultracold atomic gases, taking advantage of the fact that driving the two-body s-wave scattering length causes phenomena equivalent to isotropic fluid expansions. We specifically consider two-component fermions with contact interactions in three dimensions and discuss their dynamics under a power-law drive of the scattering length in a uniform system, employing a hydrodynamic relaxation model. We analytically solve their dynamics and find the hydrodynamic attractor solution. Our results establish the cold atom systems as a new platform for exploring hydrodynamic attractors.

Introduction.—Hydrodynamics universally describes the space-time evolution of charge densities of systems close to thermal equilibrium [1]. Hydrodynamic equations do not depend on the microscopic details of systems, which are applicable to broad fields of physics from condensed matter [2] to high-energy physics [3, 4]. Its universality is based on the coarse-graining of microscopic elements into macroscopic fluid cells. For time scales sufficiently longer than relaxation times, one can describe the dynamics of the fluid cells in terms of charge densities and their derivatives, and systematically write down hydrodynamic equations based on gradient expansions. The hydrodynamic equations at leading order in the expansion describe the ideal fluid, those up to the first order describe the Navier-Stokes fluid, and further higher-order corrections can be found as needed.

However, recent high-energy heavy-ion collision experiments reported that their initial dynamics immediately after the impact of two relativistic nuclei can be described hydrodynamically, even though it is far from equilibrium [5–9]. This "unreasonable" effectiveness of hydrodynamics triggered a reconsideration of its applicability, and suggests the existence of non-equilibrium universal attractors to hydrodynamics, which cannot be captured within naive gradient expansions in hydrodynamics [10]. Such attractors, called hydrodynamic attractors, have been actively studied and found from various microscopic theories such as hydrodynamics, kinetic theory [11], and holography [10, 12] (see review papers [13–17]).

The hydrodynamic attractor is also relevant for small systems whose typical time and length scales are comparable to their relaxation times and mean free paths. Recently, in cold atoms, such small systems were realized with the development of experimental techniques. Relaxation times of strongly interacting Fermi gases were measured through initial state preparation and time-resolved measurements, both in trapped gases [18, 19] and in uniform systems [20–22]. In particular, the detailed collective dynamics of a few strongly correlated fermions were measured [23]. These experiments make cold atomic systems an important new research platform for hydrodynamic attractors.

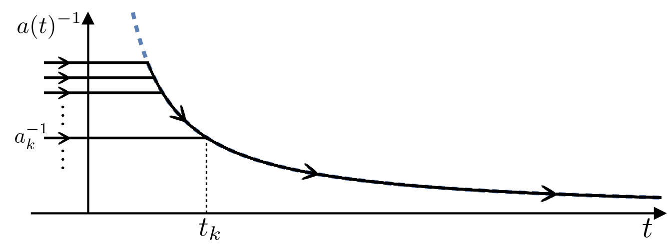

FIG. 1. Protocol for driving the scattering length to realize the hydrodynamic attractor in a uniform system without fluid velocities. The scattering length is kept at a constant value a_k up to time $t = t_k$ and then approaches the unitary limit $a^{-1}(t) \to 0$ asymptotically with a power law of time, see Eq. (11). To probe various initial conditions, the initial scattering length a_k and time t_k are varied while keeping $\tilde{a} = a_k(\tau_\zeta/t_k)^\alpha$ fixed for $k = 1, 2, 3, \ldots$ Once the drive has started for $t > t_k$, the scattering length follows a single curve.

In this Letter, we propose a setup to study hydrodynamic attractors in cold atoms. We consider a two-component Fermi gas in three dimensions whose short-range interaction is fully characterized by the two-body s-wave scattering length and discuss its hydrodynamic behavior when the scattering length is changed in time. In this system, the time variation of the scattering length at fixed volume leads to phenomena equivalent to the isotropic fluid expansions of the gas because there are no other intrinsic reference scales [24]. In other words, by temporally varying the scattering length in a uniform state without fluid velocities, one can arbitrarily drive the system out of equilibrium, equivalent to isotropic fluid expansion, while the fluid remains uniform and at rest. Taking advantage of this equivalence, we show that hydrodynamic attractors can be explored in cold atomic systems by driving the scattering length to the strongly interacting, unitary limit over time, as schematically depicted in Fig. 1.

Bulk viscosity.—Let us start with a brief review of the bulk viscosity, which characterizes dissipation in isotropic fluid expansions. According to the linear-response theory, the complex bulk viscosity $\zeta(\omega)$ at frequency ω is provided by [25–28]

$$\zeta(\omega) = \frac{\mathcal{R}_{\Pi\Pi}(\omega + i0^+) - \mathcal{R}_{\Pi\Pi}(i0^+)}{i(\omega + i0^+)}, \tag{1}$$

where $\mathcal{R}_{\Pi\Pi}(w) \equiv i\int_0^\infty \mathrm{d}t \int \mathrm{d}\boldsymbol{x}\, e^{iwt - i\boldsymbol{k}\cdot\boldsymbol{x}} \langle[\hat{\Pi}(t,\boldsymbol{x}), \hat{\Pi}(0,\boldsymbol{0})]\rangle$ is the response function of the modified trace of the stress tensor, $\hat{\Pi} \equiv \hat{\pi} - (\partial p/\partial \mathcal{N})_{\mathcal{E}}\hat{\mathcal{N}} - (\partial p/\partial \mathcal{E})_{\mathcal{N}}\hat{\mathcal{H}}$. Here, $\hat{\pi} = \sum_i \hat{\Pi}_{ii}/3$, $\hat{\mathcal{N}}$, and $\hat{\mathcal{H}}$ are the pressure operator, the number density operator, and the Hamiltonian density operator, respectively, with $p = \langle\hat{\pi}\rangle$, $\mathcal{N} = \langle\hat{\mathcal{N}}\rangle$, and $\mathcal{E} = \langle\hat{\mathcal{H}}\rangle$.

The two-component fermions with a resonant zero-range interaction are described by the Hamiltonian density [29]

$$\hat{\mathcal{H}} = \sum_{\sigma=\uparrow,\downarrow} \hat{\psi}_\sigma^\dagger \frac{-\nabla^2}{2m}\hat{\psi}_\sigma + g_0 \hat{\psi}_\uparrow^\dagger \hat{\psi}_\downarrow^\dagger \hat{\psi}_\downarrow \hat{\psi}_\uparrow, \tag{2}$$

where $\hat{\psi}_\sigma^\dagger$ is the creation operator for a fermion with spin σ. In the dimensional regularization, the coupling constant g_0 is related to the scattering length a via $g_0 = 4\pi m a$. In this system, the pressure operator satisfies

$$\hat{\pi} = \frac{2}{3}\hat{\mathcal{H}} + \frac{\hat{\mathcal{C}}}{12\pi m a}, \tag{3}$$

up to irrelevant total derivatives, with the contact density operator $\hat{\mathcal{C}} \equiv (m g_0)^2 \hat{\psi}_\uparrow^\dagger \hat{\psi}_\downarrow^\dagger \hat{\psi}_\downarrow \hat{\psi}_\uparrow$. This operator identity is the nonrelativistic counterpart of the condition of tracelessness due to conformal invariance and the second term on the right-hand side measures the breaking of the conformal symmetry. If the interaction strength is tuned to the unitary limit, i.e., $|a| = \infty$, the second term in Eq. (3) vanishes, and accordingly the equation of state obeys $p = 2\mathcal{E}/3$. In the unitary limit, therefore, the modified trace $\hat{\Pi}$ turns into zero, and the complex bulk viscosity $\zeta(\omega)$ becomes zero identically [30, 31].

Substituting the definition of the modified trace $\hat{\Pi}$ and Eq. (3) into Eq. (1), the complex bulk viscosity is expressed in terms of the response function of the contact density:

$$\zeta(\omega) = \frac{1}{(12\pi m a)^2}\frac{\mathcal{R}_{\mathcal{C}\mathcal{C}}(\omega + i0^+) - \mathcal{R}_{\mathcal{C}\mathcal{C}}(i0^+)}{i(\omega + i0^+)}, \tag{4}$$

where the commutator of the Hamiltonian and particle number operators with any operator in the grand canonical average can safely be dropped. The response function of the contact density captures how the contact density at time t changes in response to a variation of the scattering length at time $t = 0$ as

$$\langle[\hat{\mathcal{C}}(t,\boldsymbol{x}), \hat{\mathcal{C}}(0,\boldsymbol{0})]\rangle = -4\pi m \left(\frac{\partial \langle \mathcal{C}(t,\boldsymbol{x})\rangle}{\partial a(0,\boldsymbol{0})^{-1}}\right)_{S,N} \tag{5}$$

at constant entropy and particle number [28, 32]. Thus, $\zeta(\omega)$ can be measured via changes in the scattering length, as well as isotropic expansion.

At low frequencies, $\zeta(\omega)$ is well described by the Drude form of

$$\zeta(\omega) = \frac{i\chi}{\omega + i\tau_\zeta^{-1}}, \tag{6}$$

where τ_ζ is the relaxation time for the bulk viscosity that captures the details of many-body dynamics. The sum rule $\chi = (1/\pi)\int_{-\infty}^{\infty} d\omega\, \zeta(\omega) = (1 + 2/d)p - \mathcal{N}(\partial p/\partial \mathcal{N})_{\mathcal{S}}$ is a thermodynamic property [1, 33]. Both τ_ζ and χ are known analytically at high temperatures [32, 34–36] and numerically even at low temperatures in the strongly correlated fluid [32]. Although the complex bulk viscosity has a high-frequency tail proportional to $\omega^{-3/2}$ due to the short-distance singularity of the contact interaction [37, 38], this is irrelevant for the intermediate- and long-time behavior of the dynamics. More technically, the Drude form is systematically introduced by the memory function formalism [39], which has recently been successfully applied to systems without well-defined quasiparticles [40], such as the unitary Fermi gas near the critical temperature [41]. Furthermore, the Drude form is fundamental to providing a systematic and unified description for deriving the hydrodynamic equations of motion [42].

Time-dependent scattering length in hydrodynamics.— Let us consider hydrodynamically a specific situation in which the scattering length $a(t)$ is varied over time in a uniform system without fluid velocities. Then, the energy density is produced at the rate of

$$\dot{\mathcal{E}}(t) = \frac{\mathcal{C}(t)}{4\pi m a(t)^2}\dot{a}(t), \tag{7}$$

which is known as the dynamic sweep theorem [43–45]. Here, the contact density expectation value $\mathcal{C}(t)$ is divided into two parts as

$$\mathcal{C}(t) = \mathcal{C}_{\mathrm{eq}}[a(t)] + 12\pi m a(t)\pi(t), \tag{8}$$

where the first term gives the instantaneous contact density determined in thermal equilibrium with the scattering length $a(t)$, and $\pi(t)$ in the second term describes the dissipative correction to the first term in hydrodynamics.

Facilitated by the fact that complex bulk viscosity is well described by the Drude form at low frequencies, we incorporate the relaxation time $\tau_\zeta = \zeta(\omega \to 0)/\chi$ into hydrodynamics [42]. We suppose that $\pi(t)$ is given as a solution of

$$\tau_\zeta \dot{\pi}(t) + \pi(t) = -\zeta[a(t)]V_a(t), \tag{9}$$

where $\zeta[a]$ is the static bulk viscosity coefficient $\lim_{\omega\to 0}\zeta(\omega)$ for given scattering length a. Here, $V_a(t)$

is the bulk strain rate tensor modified by the time-dependent scattering length and is given by [46]

$$V_a(t) \equiv -3\partial_t \ln a(t). \tag{10}$$

Whereas the bulk strain rate tensor is given by the divergence of fluid velocities in ordinary hydrodynamics, $V_a(t)$ also has the time derivative term of the scattering length. This is a consequence of the equivalence between isotropic fluid expansion and temporal contraction of the scattering length. Remarkably, one can thus drive the fluid out of equilibrium by the scattering length and observe how it relaxes back toward equilibrium via the contact, without moving parts in a uniform system.

If we take the long-time limit $t/\tau_\zeta \to \infty$, i.e., the limit of $\tau_\zeta \to 0$, in Eq. (9), $\pi(t)$ is reduced to $\pi(t)|_{\rm NS} = -\zeta[a(t)]V_a(t)$, which gives the Navier-Stokes hydrodynamic result. Furthermore, higher-order hydrodynamic corrections beyond the Navier-Stokes level can be obtained systematically by expanding $\pi(t)$ with respect to τ_ζ. In relativistic systems, hydrodynamic equations with relaxation times in the form of Eq. (9) are commonly employed to preserve causality and are referred to as the Müller-Israel-Stewart theory [47–49].

Hydrodynamic attractor.—In order to realize the hydrodynamic attractor, we drive the scattering length to bring the system out of equilibrium. We compare several drives with different initial conditions to reveal the universal attractor in the relaxation dynamics. Specifically, we investigate the situation where the system asymptotically approaches the unitary limit by a power-law variation of the scattering length with exponent $\alpha > 0$ as

$$a_k(t)^{-1} = \begin{cases} a_k^{-1} & t < t_k, \\ a_k^{-1}(t/t_k)^{-\alpha} & t > t_k, \end{cases} \quad \text{for } k = 1, 2, \ldots \tag{11}$$

where a_k is a constant scattering length up to time t_k. Here, k is a subscript to distinguish the drives for different initial conditions. To make the drive the same at long times, we fix $a_k(\tau_\zeta/t_k)^\alpha =: \tilde{a}$, which gives the scattering length at the relaxation time in the power-law drive. Therefore, at long times, all the driving protocols lie on a single curve that asymptotically approaches the unitary limit at a power α, as shown in Figure 1.

We suppose that the system is sufficiently close to the unitary limit. Near the unitary limit, the static bulk viscosity $\zeta[a]$ is proportional to a^{-2} [50], so that we take an approximated form as $\zeta[a(t)] \simeq \zeta^{(2)}a(t)^{-2}$ with $\zeta^{(2)}$ being a constant. Then, Eq. (9) for $t > t_k$ turns into

$$\tau_\zeta \dot{\pi}(t) + \pi(t) = 3\zeta[\tilde{a}]\frac{\alpha\tau_\zeta^{2\alpha}}{t^{2\alpha+1}}, \tag{12}$$

and its analytical solution is found to be

$$\pi(t) = \pi_{\rm att}(t) + \pi_{\rm ini}e^{-t/\tau_\zeta}, \tag{13}$$

where $\pi_{\rm ini} = -e^{t_k/\tau_\zeta}\pi_{\rm att}(t_k)$ is determined from the initial condition $\pi(t_k) = 0$ because the system is in equilibrium with a constant scattering length up to time $t = t_k$. Here, $\pi_{\rm att}(t)$ is given by

$$\pi_{\rm att}(t) = \frac{3\zeta[\tilde{a}]\alpha}{\tau_\zeta}(-1)^{2\alpha+1}e^{-t/\tau_\zeta}\Gamma(-2\alpha, -t/\tau_\zeta), \tag{14}$$

with $\Gamma(s,x)$ being the incomplete Gamma function [51]. The first term of Eq. (13), $\pi_{\rm att}(t)$, depends on a_k and t_k not separately but only through the fixed parameter $\tilde{a}$, while the second term explicitly depends on t_k. Therefore, $\pi_{\rm att}(t)$ is independent of the initial condition.

Let us investigate the behavior of the solution $\pi(t)$ in the long-time limit, where the Navier-Stokes hydrodynamics have to be reproduced. The first term $\pi_{\rm att}(t)$ is expanded for long times $t \gg \tau_\zeta$ as

$$\pi_{\rm att}(t) = 3\zeta[\tilde{a}]\frac{\alpha\tau_\zeta^{2\alpha}}{t^{2\alpha+1}}\left[1 + (2\alpha+1)\frac{\tau_\zeta}{t} + O\left((\tau_\zeta/t)^2\right)\right], \tag{15}$$

where the exponential factor e^{-t/τ_ζ} in Eq. (14) is harmless in the expansion with respect to t/τ_ζ due to the asymptotic behavior of the incomplete Gamma function, $\Gamma(-s,-z) = (-1/z)^{s+1}e^z/\Gamma(s+1)\sum_{n=0}^{\infty}\Gamma(s+n+1)z^{-n}$ for $|z| \to \infty$. In this expansion, the first term coincides with the Navier-Stokes result, and the second term gives a second-order hydrodynamic correction. In contrast, the initial condition in the second term in Eq. (13) has an exponential damping factor $e^{-(t-t_k)/\tau_\zeta}$, which cannot be expanded with respect to τ_ζ/t, and is called the non-hydrodynamic mode.

The key point is that the expansion (15) is asymptotic with convergence radius zero. The coefficient of the n th-order term in the expansion is, indeed, proportional to $\Gamma(2\alpha + n + 1)$ and diverges factorially. This factorial divergence makes the gradient expansion underlying hydrodynamics a divergent series and significantly less accurate for small t/τ_ζ. On the other hand, $\pi_{\rm att}(t)$ itself, given analytically in Eq. (14), universally describes the system accurately, independent of the initial conditions, for $t/\tau_\zeta \gtrsim 1$ after the non-hydrodynamic mode has decayed exponentially. Because the universality emerges before the time scale $t \gg \tau_\zeta$ at which hydrodynamics becomes accurate, $\pi_{\rm att}(t)$ is called *the hydrodynamic attractor*.

Note that while we have found $\pi_{\rm att}(t)$ as the exact solution of Eq. (12), it can also be obtained from the Borel summation of the expansion (15) [52]. In other words, $\pi_{\rm att}(t)$ has a non-analytic contribution, which cannot be directly captured in the expansion (15). For example, the attractor solution for $\alpha = 1/2$ is expanded for short times $t \ll \tau_\zeta$ as

$$\pi_{\rm att}(t)|_{\alpha=1/2} = \frac{3\zeta[\tilde{a}]}{2\tau_\zeta}\left[-\frac{\tau_\zeta}{t} + \gamma + \ln\frac{t}{\tau_\zeta} + O(t/\tau_\zeta)\right], \tag{16}$$

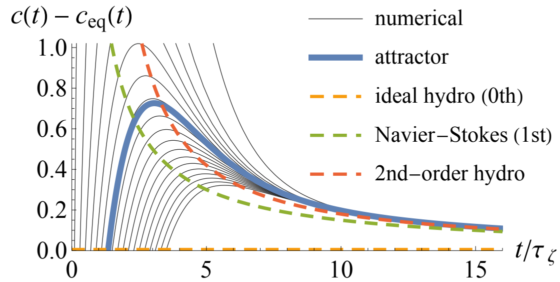

FIG. 2. The hydrodynamic attractor solution (blue thick line) for the deviation of the dimensionless contact density from its equilibrium value, $c(t) - c_{\rm eq}[a(t)] \equiv (\mathcal{C}(t) - \mathcal{C}_{\rm eq}[a(t)])/(12\pi m a(t)) \times (\tau_\zeta/\zeta[a(t)])$, as a function of t/τ_ζ under the drive with a power $\alpha = 1/2$. We also plot numerical solutions (black thin lines) of Eq. (13) for $t_k/\tau_\zeta = 0.1, 0.3, 0.5, \ldots, 3.5$ and hydrodynamic results of zeroth-order, first-order, and second-order (orange, green, and red dashed line, respectively) from the expansion (15). The universal attractor solution corresponds to the numerical solution with $t_k/\tau_\zeta = 1.347\ldots$

with $\gamma = 0.5772\ldots$ being Euler's constant. The Borel summation for effective theories is one of the common approaches to finding the hydrodynamic attractors [10].

Contact density.—Figure 2 plots the deviation of the dimensionless contact density $c(t) \equiv \mathcal{C}(t)/(12\pi m a(t)) \times (\tau_\zeta/\zeta[a(t)])$ from its instantaneous value under the drive of the scattering length with a power $\alpha = 1/2$. Here, the dimensionless contact density does not depend on the fixed parameter $\tilde{a}$. Numerical solutions of Eq. (12) for $t_k/\tau_\zeta = 0.1, 0.3, \ldots, 3.5$ (black thin lines) remain zero (their equilibrium values) until the start of driving at $t = t_k$, and then take positive values as shown in Fig. 2. Importantly, the numerical solutions converge immediately to the universal attractor solution (blue thick line) before being reduced to the hydrodynamic solutions (dashed lines).

From the perspective of the Navier-Stokes solution, the attractor appears to result from an effective bulk viscosity coefficient that varies at short times before it approaches its equilibrium value at long times. The effective bulk viscosity coefficient $\zeta^{(\alpha)}_{\rm eff}[a(t)]$ can be defined for $t > t_k$ by representing the hydrodynamic attractor solution in the form of the Navier-Stokes result [12]:

$$\pi_{\rm att}(t) = 3\zeta^{(\alpha)}_{\rm eff}[a(t)]\frac{\alpha}{t}. \tag{17}$$

From the explicit form of the attractor solution (14), we find

$$\frac{\zeta^{(\alpha)}_{\rm eff}[a(t)]}{\zeta[a(t)]} = \left(-\frac{t}{\tau_\zeta}\right)^{2\alpha+1} e^{-t/\tau_\zeta}\Gamma(-2\alpha, -t/\tau_\zeta). \tag{18}$$

The effective viscosity $\zeta^{(\alpha)}_{\rm eff}[a(t)]$ has non-analytic contributions in the expansion with respect to t/τ_ζ, analogous to the short-time expansion of $\pi_{\rm att}(t)$ in Eq. (16).

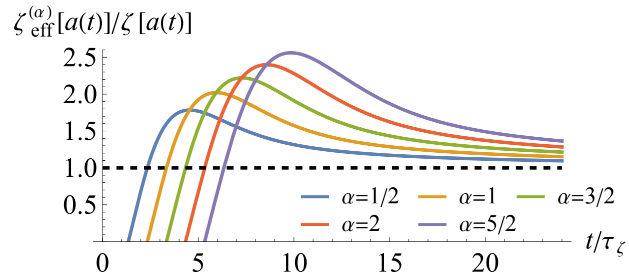

FIG. 3. The effective, time-dependent bulk viscosity coefficients reproduce the attractor solution when inserted into the Navier-Stokes dynamics (18); shown here for different drive exponents α.

Figure 3 plots the effective bulk viscosity as a function of t/τ_ζ for various powers. Since the ratio (18) measures the deviation of the attractor solution from the Navier-Stokes result, it asymptotically approaches unity in the long-time limit. The ratio has a peak for intermediate times and is suppressed for short times. These tendencies are generally found in the effective viscosity coefficients defined by the hydrodynamic attractor [12].

Discussion and outlook.—In this Letter, we have proposed a driving protocol of the scattering length to observe the hydrodynamic attractor in cold atoms; this protocol is given by Eq. (11) and schematically depicted in Fig. 1. Employing the hydrodynamic equation with the relaxation time [Eq. (9)], we have analytically found the attractor solution and the non-hydrodynamic mode as Eq. (13). The dynamics of the contact density in our protocol is plotted in Fig. 2, where the solutions from different initial conditions converge to the attractor solution already before the time scale where the hydrodynamics become relevant. Similarly, one can find the dynamics of other thermodynamic variables such as the energy density by integrating Eq. (7). The deviation between the attractor solution and the Navier-Stokes solution is measured as the ratio of the effective viscosity coefficient in Eq. (18) and Fig. 3. Since we can choose the power α arbitrarily, these results would be useful for measuring the bulk viscosity coefficient $\zeta[a]$ near the unitary limit, or more precisely $\zeta^{(2)}$.

Since our analysis neglects the high-frequency tail of the correlation function due to the singularity of the short-range interaction, the short-time behavior of our results is not exact. However, the details near the initial time immediately disappear as non-hydrodynamic modes, and the dynamics universally follow the attractor solution for intermediate and long times. On the other hand, the power-law drive at a power $\alpha = 1/2$ leads to another universality in the short-time dynamics due to the scale invariance ($t \to \lambda^2 t$ and $\boldsymbol{x} \to \lambda\boldsymbol{x}$) of the zero-density nonrelativistic system [53]. It will be worthwhile to explore how this short-time universality and the intermediate- and long-time universality of the hydrodynamic attractor can be connected.

It is also worthwhile to remark that our proposed protocol is analogous to a relativistic hydrodynamic attractor in a Hubble expansion [54]. This is because the time variation of the scattering length corresponds to the variation of the spatial metric. Therefore, it is significant to explore hydrodynamic attractors in cold atom systems, where the initial-time dynamics can be directly observed, unlike in heavy-ion collision experiments. Specifically, the scattering length can be tuned by changes in the magnetic field [55], while the contact dynamics have been measured with high resolution in time [56]. In particular, our proposed protocol allows the choice of arbitrary power of the driving and, moreover, allows various initial states to be realized in a well-controlled manner.

The authors thank A. Mazeliauskas and J. H. Thywissen for useful discussions, particularly at the EMMI Rapid Reaction Task Force "Deciphering many-body dynamics in mesoscopic quantum gases." This work is supported by the Deutsche Forschungsgemeinschaft (DFG, German Research Foundation), project-ID 273811115 (SFB1225 ISOQUANT), and under Germany's Excellence Strategy EXC2181/1-390900948 (the Heidelberg STRUCTURES Excellence Cluster). K.F. is supported by JSPS KAKENHI Grant Number JP24KJ0062.

* k.fujii@phys.s.u-tokyo.ac.jp

[1] L. D. Landau and E. M. Lifshitz, *Fluid mechanics*, Vol. 6 (Butterworth-Heinemann, Oxford, 1987).
[2] P. M. Chaikin and T. C. Lubensky, *Principles of Condensed Matter Physics* (Cambridge University Press, Cambridge, UK, 2000).
[3] D. H. Rischke, Hydrodynamics and collective behaviour in relativistic nuclear collisions, Nucle. Phys. A **610**, 88 (1996).
[4] M. Vogelsberger, S. Genel, V. Springel, P. Torrey, D. Sijacki, D. Xu, G. Snyder, S. Bird, D. Nelson, and L. Hernquist, Properties of galaxies reproduced by a hydrodynamic simulation, Nature **509**, 177 (2014).
[5] V. Khachatryan *et al.* (CMS), Observation of Long-Range Near-Side Angular Correlations in Proton-Proton Collisions at the LHC, JHEP **09**, 091.
[6] B. Abelev *et al.* (ALICE), Long-range angular correlations on the near and away side in p-Pb collisions at $\sqrt{s_{NN}} = 5.02$ TeV, Phys. Lett. B **719**, 29 (2013).
[7] G. Aad *et al.* (ATLAS), Observation of Associated Near-Side and Away-Side Long-Range Correlations in $\sqrt{s_{NN}}$=5.02 TeV Proton-Lead Collisions with the ATLAS Detector, Phys. Rev. Lett. **110**, 182302 (2013).
[8] C. Aidala *et al.* (PHENIX), Creation of quark–gluon plasma droplets with three distinct geometries, Nat. Phys. **15**, 214 (2019).
[9] M. I. Abdulhamid *et al.* (STAR), Measurements of the Elliptic and Triangular Azimuthal Anisotropies in Central He3+Au, d+Au and p+Au Collisions at sNN=200 GeV, Phys. Rev. Lett. **130**, 242301 (2023).
[10] M. P. Heller and M. Spaliński, Hydrodynamics beyond the gradient expansion: Resurgence and resummation, Phys. Rev. Lett. **115**, 072501 (2015).
[11] A. Kurkela, A. Mazeliauskas, J.-F. Paquet, S. Schlichting, and D. Teaney, Matching the nonequilibrium initial stage of heavy ion collisions to hydrodynamics with QCD kinetic theory, Phys. Rev. Lett. **122**, 122302 (2019).
[12] P. Romatschke, Relativistic Fluid Dynamics Far From Local Equilibrium, Phys. Rev. Lett. **120**, 012301 (2018).
[13] P. Romatschke, Relativistic hydrodynamic attractors with broken symmetries: non-conformal and non-homogeneous, JHEP **12**, 079.
[14] W. Florkowski, M. P. Heller, and M. Spaliński, New theories of relativistic hydrodynamics in the LHC era, Rep. Progr. Phys. **81**, 046001 (2018).
[15] P. Romatschke and U. Romatschke, Relativistic fluid dynamics in and out of equilibrium – ten years of progress in theory and numerical simulations of nuclear collisions (2019), arXiv:1712.05815 [nucl-th].
[16] J. Berges, M. P. Heller, A. Mazeliauskas, and R. Venugopalan, QCD thermalization: Ab initio approaches and interdisciplinary connections, Rev. Mod. Phys. **93**, 035003 (2021).
[17] A. Soloviev, Hydrodynamic attractors in heavy ion collisions: a review, Eur. Phys. J. C **82** (2022).
[18] E. Vogt, M. Feld, B. Fröhlich, D. Pertot, M. Koschorreck, and M. Köhl, Scale invariance and viscosity of a two-dimensional Fermi gas, Phys. Rev. Lett. **108**, 070404 (2012).
[19] J. Brewer and P. Romatschke, Nonhydrodynamic transport in trapped unitary Fermi gases, Phys. Rev. Lett. **115**, 190404 (2015).
[20] P. B. Patel, Z. Yan, B. Mukherjee, R. J. Fletcher, J. Struck, and M. W. Zwierlein, Universal sound diffusion in a strongly interacting Fermi gas, Science **370**, 1222 (2020).
[21] X. Li, X. Luo, S. Wang, K. Xie, X.-P. Liu, H. Hu, Y.-A. Chen, X.-C. Yao, and J.-W. Pan, Second sound attenuation near quantum criticality, Science **375**, 528 (2022).
[22] X. Li, J. Huang, and J. E. Thomas, Universal Hydrodynamic Transport Times in the Normal Phase of a Unitary Fermi Gas (2024), arXiv:2402.14104 [cond-mat.quant-gas].
[23] S. Brandstetter, P. Lunt, C. Heintze, G. Giacalone, L. H. Heyen, M. Gałka, K. Subramanian, M. Holten, P. M. Preiss, S. Floerchinger, and S. Jochim, Emergent hydrodynamic behaviour of few strongly interacting fermions (2023), arXiv:2308.09699 [cond-mat.quant-gas].
[24] K. Fujii and Y. Nishida, Hydrodynamics with spacetime-dependent scattering length, Phys. Rev. A **98**, 063634 (2018).
[25] H. Mori, Collective Motion of Particles at Finite Temperatures, PTEP **28**, 763 (1962).
[26] J. M. Luttinger, Theory of thermal transport coefficients, Phys. Rev. **135**, A1505 (1964).
[27] B. Bradlyn, M. Goldstein, and N. Read, Kubo formulas for viscosity: Hall viscosity, Ward identities, and the relation with conductivity, Phys. Rev. B **86**, 245309 (2012).
[28] K. Fujii and Y. Nishida, Bulk viscosity of resonating fermions revisited: Kubo formula, sum rule, and the dimer and high-temperature limits, Phys. Rev. A **102**, 023310 (2020).
[29] W. Zwerger, ed., *The BCS–BEC Crossover and the Unitary Fermi Gas*, Lecture Notes in Physics Vol. 836 (Springer, Berlin, Heidelberg, 2012).

[30] Y. Nishida and D. T. Son, Nonrelativistic conformal field theories, Phys. Rev. D **76**, 086004 (2007).

[31] D. T. Son, Vanishing bulk viscosities and conformal invariance of the unitary fermi gas, Phys. Rev. Lett. **98**, 020604 (2007).

[32] T. Enss, Bulk Viscosity and Contact Correlations in Attractive Fermi Gases, Phys. Rev. Lett. **123**, 205301 (2019).

[33] E. Taylor and M. Randeria, Apparent low-energy scale invariance in two-dimensional Fermi gases, Phys. Rev. Lett. **109**, 135301 (2012).

[34] Y. Nishida, Viscosity spectral functions of resonating fermions in the quantum virial expansion, Ann. Phys. **410**, 167949 (2019).

[35] J. Hofmann, High-temperature expansion of the viscosity in interacting quantum gases, Phys. Rev. A **101**, 013620 (2020).

[36] K. Fujii and T. Enss, Bulk viscosity of resonantly interacting fermions in the quantum virial expansion, Ann. Phys. **453**, 169296 (2023).

[37] J. Hofmann, Current response, structure factor and hydrodynamic quantities of a two- and three-dimensional Fermi gas from the operator-product expansion, Phys. Rev. A **84**, 043603 (2011).

[38] W. D. Goldberger and Z. U. Khandker, Viscosity sum rules at large scattering lengths, Phys. Rev. A **85**, 013624 (2012).

[39] W. Götze and P. Wölfle, Homogeneous dynamical conductivity of simple metals, Phys. Rev. B **6**, 1226 (1972).

[40] S. A. Hartnoll, A. Lucas, and S. Sachdev, *Holographic Quantum Matter* (MIT press, Cambridge, MA, 2018).

[41] B. Frank, W. Zwerger, and T. Enss, Quantum critical thermal transport in the unitary Fermi gas, Phys. Rev. Res. **2**, 023301 (2020).

[42] D. Forster, *Hydrodynamic Fluctuations, Broken Symmetry and Correlation Functions* (WA Benjamin, 1975).

[43] S. Tan, Energetics of a strongly correlated Fermi gas, Ann. of Phys. **323**, 2952 (2008).

[44] S. Tan, Large momentum part of a strongly correlated Fermi gas, Ann. of Phys. **323**, 2971 (2008).

[45] S. Tan, Generalized virial theorem and pressure relation for a strongly correlated Fermi gas, Ann. of Phys. **323**, 2987 (2008).

[46] In Ref. [24], the bulk strain rate tensor with a spacetime dependent scattering length is generally derived as $V_a(t,\boldsymbol{x}) = \nabla\cdot\boldsymbol{v}(t,\boldsymbol{x}) - 3[\partial_t \ln a(t,\boldsymbol{x}) + \boldsymbol{v}(t,\boldsymbol{x})\cdot\nabla \ln a(t,\boldsymbol{x})]$, where $\boldsymbol{v}(t,\boldsymbol{x})$ is the fluid velocity and $a(t,\boldsymbol{x})$ is the spacetime dependent scattering length. In uniform systems without fluid velocities, the bulk strain rate tensor is given only by the time derivative term of the scattering length.

[47] I. Müller, Zum Paradoxon der Wärmeleitungstheorie, Z. Phys. **198**, 329 (1967).

[48] W. Israel, Nonstationary irreversible thermodynamics: A causal relativistic theory, Ann. Phys. **100**, 310 (1976).

[49] W. Israel and J. Stewart, Transient relativistic thermodynamics and kinetic theory, Ann. Phys. **118**, 341 (1979).

[50] K. Dusling and T. Schäfer, Bulk Viscosity and Conformal Symmetry Breaking in the Dilute Fermi Gas near Unitarity, Phys. Rev. Lett. **111**, 120603 (2013).

[51] The incomplete Gamma function $\Gamma(-s,-x)$ for $s > 0$ and $x > 0$ appears from the integral $\int_{x_0}^{x} dt\, e^t t^{-s-1} = (-1)^{s+1}[\Gamma(-s,-x) - \Gamma(-s,-x_0)]$ and formally describes the general solution independent of the initial conditions for the hydrodynamic equation (12).

[52] See Supplemental Material for the derivation of the attractor solution from the Borel summation of an expanded solution in the long-time limit.

[53] R. Qi, Z. Shi, and H. Zhai, Maximum energy growth rate in dilute quantum gases, Phys. Rev. Lett. **126**, 240401 (2021).

[54] Z. Du, X.-G. Huang, and H. Taya, Hydrodynamic attractor in a Hubble expansion, Phys. Rev. D **104**, 056022 (2021).

[55] C. Chin, R. Grimm, P. Julienne, and E. Tiesinga, Feshbach resonances in ultracold gases, Rev. Mod. Phys. **82**, 1225 (2010).

[56] C. Luciuk, S. Smale, F. Böttcher, H. Sharum, B. A. Olsen, S. Trotzky, T. Enss, and J. H. Thywissen, Observation of quantum-limited spin transport in strongly interacting two-dimensional Fermi gases, Phys. Rev. Lett. **118**, 130405 (2017).

[57] I. Aniceto, G. Başar, and R. Schiappa, A primer on resurgent transseries and their asymptotics, Physics Reports **809**, 1 (2019).

Supplemental Materials:
Hydrodynamic Attractor in Ultracold Atoms

Derivation of the attractor solution from the Borel summation

Definition of the Borel summation

We consider a formal power series:

$$A(z) = \sum_{n=0}^{\infty} a_n z^n, \tag{S1}$$

where a_n is a real constant. Here, $A(z)$ is supposed not necessarily to converge. For later convenience, we assume that the coefficient a_n has a factorial factor proportional to $\Gamma(n+p+1)$ for $p \in \mathbb{R}$, rather than the usual factorial factor $\Gamma(n+1)$. Let us introduce the Borel transform of $A(z)$ as

$$\mathcal{B}_p[A](s) \equiv \sum_{n=0}^{\infty} \frac{a_n}{\Gamma(n+p+1)} s^{n+p}. \tag{S2}$$

Then, the Borel summation of $A(z)$ is defined as

$$\mathcal{S}_p[A](z) \equiv \mathrm{P}\int_0^{\infty} ds\, e^{-s} z^{-p} \mathcal{B}_p[A](sz), \tag{S3}$$

where P represents the principal value. Note that the definitions of the Borel transform and the Borel summation here are slightly extended from the usual definitions with $p = 0$ because of the factorial factor $\Gamma(n+p+1)$ of the coefficient a_n.

The Borel transform $\mathcal{B}_p[A](s)$ of a series $A(z)$ can have singularities at $s > 0$. When a series $A(z)$ is given as a perturbative solution of a certain problem with a small parameter z, the singularities of the Borel transform $\mathcal{B}_p[A](s)$ correspond to non-perturbative contributions, which are not captured in the expansion with respect to z such as $e^{-1/z}$ [57]. However, such non-perturbative contributions are irrelevant as they correspond to non-hydrodynamic modes for our purposes focusing on hydrodynamic attractors. Thus, we take the principal value in the definition of the Borel summation $\mathcal{S}_p[A](z)$ as a simple method to avoid the singularities.

Expanded solution of Eq. (12)

Based on the perspective of gradient expansions in hydrodynamics, we solve Eq. (12) by expanding $\pi(t)$ with respect to τ_ζ/t, which is small in the long-time limit. By factoring out the trivial prefactor $3\zeta[\tilde{a}]\alpha\tau_\zeta^{2\alpha}/t^{2\alpha+1}$ corresponding to the right-hand side of Eq. (12), we expand $\pi(t)$ as

$$\pi(t) = 3\zeta[\tilde{a}]\frac{\alpha\tau_\zeta^{2\alpha}}{t^{2\alpha+1}}\tilde{\pi}(\tau_\zeta/t), \qquad \tilde{\pi}(z) = \sum_{n=0}^{\infty} \pi_n z^n. \tag{S4}$$

Substituting this expansion into Eq. (12), we find

$$\pi_n = \frac{\Gamma(2\alpha+n+1)}{\Gamma(2\alpha+1)} \qquad \text{for} \quad n = 0, 1, 2, \ldots, \tag{S5}$$

where the coefficients are determined independently of the initial condition for $\pi(t)$. Here, the leading-order solution coincides with the Navier-Stokes hydrodynamic result, and the n th-order solution gives the $(n+1)$ th-order hydrodynamic correction. Importantly, since π_n is proportional to $\Gamma(2\alpha+n+1)$ and diverges factorially, the expansion (S4) does not converge. Nevertheless, we can obtain a meaningful result for $\pi(t)$ involving information up to infinite order using the aforementioned Borel summation.

Borel summation of $\pi(t)$

The Borel transform of $\tilde{\pi}(z)$ is computed as

$$\mathcal{B}_{2\alpha}[\tilde{\pi}](s) = \sum_{n=0}^{\infty} \frac{\pi_n}{\Gamma(n+2\alpha+1)} s^{n+2\alpha} = \frac{1}{\Gamma(2\alpha+1)} \frac{s^{2\alpha}}{1-s}. \tag{S6}$$

Although the summation in the Borel transform converges only for $|s| < 1$, its defined domain can be extended to $s \in \mathbb{C}$ except for $s = 1$ by an analytic continuation. Subsequently, its Borel summation is computed as

$$\mathcal{S}_{2\alpha}[\tilde{\pi}](z) = \frac{1}{\Gamma(2\alpha+1)} \mathrm{P}\int_0^{\infty} ds\, e^{-s} \frac{s^{2\alpha}}{1-sz} = e^{-1/z}(-z)^{-2\alpha-1}\Gamma(-2\alpha, -z^{-1}). \tag{S7}$$

Therefore, the corresponding Borel summation of $\pi(t)$ is obtained as

$$\pi_{\mathrm{Borel}}(t) = 3\zeta[\tilde{a}] \frac{\alpha \tau_\zeta^{2\alpha}}{t^{2\alpha+1}} \mathcal{S}_{2\alpha}[\tilde{\pi}](\tau_\zeta/t) = 3\zeta[\tilde{a}] \frac{\alpha}{\tau_\zeta} (-1)^{2\alpha+1} e^{-t/\tau_\zeta} \Gamma(-2\alpha, -t/\tau_\zeta), \tag{S8}$$

which is identical to the attractor solution (14) in the main text.